Coulomb Excitation and Reorientation of the Octupole State in ^{208}Pb†

A. R. BARNETT AND W. R. PHILLIPS*
J. H. Williams Laboratory, University of Minnesota, Minneapolis, Minnesota 55455
(Received 21 April 1969)

The static quadrupole moment (Q) of the 2.614-MeV 3^- level in ^{208}Pb has been measured by observing the angular distribution of inelastically scattered ^{4}He and ^{16}O ions following $E3$ Coulomb excitation. The reduced matrix element for the $E3$ transition from the ground state to the 3^- state, $B(E3)\uparrow$, was also obtained. Distributions were taken over the range 80°–170°, using a multiple solid-state-detector array, at α-particle energies of 19, 18, and 17.5 MeV, and at an oxygen energy of 69.1 MeV. Differential inelastic cross sections were in the range 10–40 μb/sr for α's and 200–300 μb/sr for oxygen. The 19-MeV data showed strong interference between the Coulomb-excitation amplitude and an amplitude resulting from direct nuclear excitation. The remaining three sets of data showed no such interference and were analyzed simultaneously using the symmetrized semiclassical Coulomb-excitation theory of Alder *et al.*: The fitted parameters $B(E3)\uparrow$ and Q are correlated, with best-fit values of $B(E3)\uparrow = 0.58\pm0.04$ e^2 b^3 and $Q = -1.3\pm0.6$ b. The α data are not very sensitive to Q and yet are essential to the result, for the analysis of the α and oxygen data together limits the acceptable parameter range much more than if the oxygen data alone are used.

I. INTRODUCTION

OVER the past few years many experiments have appeared whose aim has been the measurement of static quadrupole moments of the first excited 2^+ states in even-even nuclei.[1] The method used in these experiments has been to try to observe second-order effects that may occur when the levels are Coulomb excited,[2–4] an example being the deviation of the angular distribution of the inelastically scattered particles causing the excitations from the first-order prediction. The differing results of several experiments[1,5] suggest that one must treat with reserve the various numbers for the quadrupole moments and their reliability estimates. It should be reemphasized[3] that these Coulomb-excitation "reorientation" experiments must be done over a considerable range of angles, energies, and bombarding conditions if reliable Q's are to be extracted from them. In particular, bombarding energies well below supposed Coulomb barriers have to be used in order that no amplitude other than that due to electric Coulomb excitation be involved in the inelastic exit channel and in order that the simplest interpretation of the semiclassical Coulomb excitation theory[4] be valid.

Despite the difficulties, reorientation experiments can provide reliable values for quadrupole moments. Thus, for instance, there is evidence that the moments of several one-phonon 2^+ levels in the so-called spherical vibrational nuclei are nonzero[1,5]; their absolute values give information on anharmonicities in the vibrations within a macroscopic model[6] and valuable numbers for comparison with predictions of microscopic-model wave functions.[7]

No reorientation experiments exist for the one-phonon 3^- vibrational levels of nuclei excited by $E3$ Coulomb excitation; indeed, few $E3$ Coulomb-excitation experiments have been done at all.[8] The doubly closed shell nucleus ^{208}Pb has as its first state the 3^- octupole vibration at 2.614 MeV. There exist several microscopic calculations of the wave function of the 3^- level based on particle-hole excitations of the core,[9] and a measurement of the quadrupole moment of that state would be of some interest. In this paper we report on such a measurement, which is based on observation of the Coulomb excitation of that level.

The differential cross sections for the inelastic scattering of α particles to the 3^- state in ^{208}Pb were measured at bombarding energies of 19, 18, and 17.5 MeV, and for the inelastic scattering of ^{16}O ions at an energy of 69.1 MeV. The experimental techniques used are discussed in Sec. II. Evidence is presented that at the lowest two α-particle bombarding energies we are dealing with Coulomb excitation alone. At 19 MeV, there is interference from nuclear effects, although 19 MeV is a bombarding energy below most prescriptions (e.g., Ref. 1) for "safe" Coulomb-excitation experiments, and proportionally as far below the "Coulomb barrier" as other experiments[1] that have attempted to measure

† Supported in part by the U.S. Atomic Energy Commission.
* On leave from the University of Manchester, Manchester 13, England.

[1] J. de Boer and J. Eichler, in *Advances in Nuclear Physics*, edited by M. Baranger and E. Vogt (Plenum Press, Inc., New York, 1967), Vol. I, p. 1; see also Refs. 17–19.
[2] K. Alder and A. Winther, *Coulomb Excitation* (Academic Press Inc., New York, 1966); and Ref. 30.
[3] G. Breit, R. L. Gluckstern, and J. E. Russell, Phys. Rev. **103**, 727 (1956).
[4] K. Alder, A. Bohr, T. Huus, B. Mottelson, and A. Winther, Rev. Mod. Phys. **28**, 432 (1956).
[5] R. G. Stokstad, I. Hall, G. D. Symons, and J. de Boer, Nucl. Phys. **A92**, 319 (1967); J. J. Simpson, D. Eccleshall, M. J. L. Yates, and N. J. Freeman, *ibid.* **A94**, 177 (1967); and Ref. 17.
[6] See, for example, K. Kumar and M. Baranger, Nucl. Phys. **A92**, 608 (1967).
[7] See, for example, M. Baranger and K. Kumar, Nucl. Phys. **A122**, 273 (1968).
[8] G. A. Jones and W. R. Phillips, Proc. Roy. Soc. (London) **A239**, 487 (1957); O. Hansen and O. Nathan, Nucl. Phys. **42**, 197 (1963); T. K. Alexander, O. Häusser, K. W. Allen, and A. E. Litherland, Bull. Am. Phys. Soc. **14**, 123 (1969).
[9] V. Gillet, A. M. Green, and E. A. Sanderson, Nucl. Phys. **88**, 321 (1966); and Refs. 42 and 43.

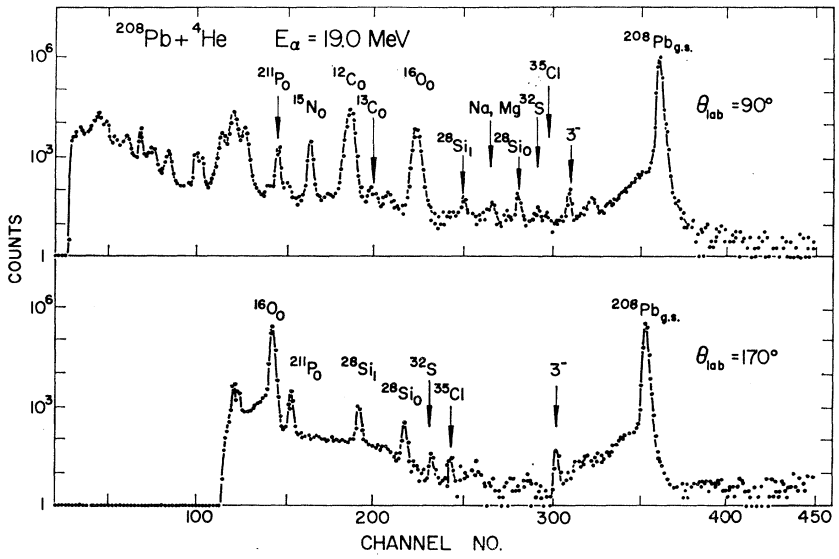

FIG. 1. Two of eight simultaneous α spectra taken at 19-MeV α energy. Various peaks from light contaminants are indicated, as well as the inelastic α scattering to the 3^- state of ^{208}Pb, and the α decay following the reaction ^{208}Pb$(\alpha, n)^{211}$Po(7.45 MeVα)^{207}Pb. General background-to-peak ratios were about 2×10^{-5}:1 in the region of the 3^- peak. The target thickness was 144 μg/cm^2 of 99.7% ^{208}Pb on 10 μg/cm^2 carbon.

fine details from Coulomb excitation. With the 69.1-MeV ^{16}O ions no effects other than Coulomb excitation and nucleon tunnelling are believed to be taking place. The three sets of electric excitation data (α's at 18 and 17.5 MeV, ^{16}O at 69 MeV) were analyzed together using the symmetrized semiclassical theory of Coulomb excitation reviewed by Alder *et al.*[4] The theory involved is discussed in Sec. III where it is shown that the only second-order paths that contribute significantly to the observed deviations of the cross sections from the first-order perturbation theory expressions are those involving reorientations among the magnetic substates of the 3^- level itself. (This is true only in special cases such as ^{208}Pb which has a relatively isolated first excited 3^- state.) Thus the first-order cross section $d\sigma^{(1)}$ needs correction, to good approximation, only by a term $d\sigma^{(1,2)}$ proportional to the quadrupole moment Q, and hence the analysis of the α and ^{16}O data yields values of Q and $B(E3)$, the reduced matrix element for the upward $E3$ transition.

The use of the semiclassical theory to predict the cross sections is probably valid, since the Sommerfeld parameter η is roughly 12 in the α experiments, and 50 in the ^{16}O experiments. The procedure adopted to symmetrize the semiclassical expressions is discussed later in Sec. III. Calculations[10] on the validity of the symmetrized semiclassical theory for $E2$ reorientation experiments show that the corrections from a full quantal treatment are negligible if η is greater than about 5. We assume in the $E3$ case that for our values of η the theory we use gives an adequate description.

In Sec. IV the details of the analysis of each of the data sets are presented. In Sec. V we discuss the results obtained and their uncertainties. The value of $B(E3)$ obtained is compared with previous experimental values for this quantity, and the value of Q obtained is compared with model wave-function predictions.

II. EXPERIMENTAL TECHNIQUE

The Emperor Tandem at the Williams Laboratory was used to produce α beams of up to 1 μA ^{4}He^{2+} and oxygen beams of 200 nA ^{16}O^{6+} on target. Silicon surface-barrier detectors were used to measure the elastic and the inelastic scattering for both the α and the oxygen data. The detectors had depletion depths of 600 μ at 100-V bias and were stopped down to 0.25-in. diam by 10-mil stainless-steel defining apertures. The solid angle subtended by each detector was 1.008 msr with individual variations of up to 0.3%. The detectors were mounted in a precision ring fitted to an Ortec scattering chamber and could be positioned with an angular accuracy of 0.1°. Tests with detectors on opposite sides of the beam showed that experimental asymmetries were $<0.3\%$. Eight detectors were used to take the 19-MeV α data and the pulses were routed into four analog-to-digital converters (ADC's). For the remainder of the experiment, six detectors and six ADC's were used. There are several advantages to the multiple-detector system over other methods of measuring the inelastic scattering, a major one being that even with the low cross sections, the data could be accumulated in a reasonable time. There was no magnetic analysis of the reaction products, and so no corrections were needed for variations in the charge-state populations of the outgoing ions. A further advantage is that the effect of beam movements over possible target nonuniformities was largely eliminated.

The targets used were evaporated from 99.7% enriched ^{208}Pb onto 10–20-μg/cm^2 carbon foils. A thickness of 144 μg/cm^2 was used for the α runs and 59 μg/cm^2 for the oxygen runs; these were, respectively,

[10] U. Smilansky, Nucl. Phys. **A112**, 185 (1968).

TABLE I. Summary of some experimental details for the α and oxygen Coulomb-excitation measurements on the 3^- state of ^{208}Pb at 2.614 MeV.

Energy (MeV)	Ion	Charge[a] (mC)	Average beam (nA)	Target thickness[b] (μg/cm^2)	Energy loss (keV)	$\sigma_{\text{Total}}(\alpha, n)$[c] (mb)
19.0	$^4He^{2+}$	10	250	54 144	16	7.8±0.4
18.0	$^4He^{2+}$	9	300	144	16	1.8±0.3
17.5	$^4He^{2+}$	26	1000	144	16	0.8±0.1
69.1	$^{16}O^{6+}$	20	200[d]	59	112	...

[a] Approximate total charge for each datum point, with 6–8 angles measured simultaneously.

[b] Assuming Rutherford scattering (see Fig. 6) and a mean charge of the Faraday cup of 2^+ and 8^+ for α and ^{16}O.

[c] The errors quoted are statistical only and do not allow for possible systematic losses, e.g., ^{211}Po ions that leave the target.

[d] Limited by energy dissipation in target.

16 and 112 keV thick to the beam. No target deterioration was observed after many hours of bombardment. The target thicknesses were estimated from the Rutherford cross section (see, however, Fig. 6), the known solid angle, and charge. The mean-charge states in the Faraday cup were taken to be 2+ and 8+, although that for ^{16}O was somewhat less. The current integrator used (BNI model 1000) was accurate to 0.1% but it was used only to monitor and check different runs and targets, thus no measurements were needed of the charge-state distribution of the beam or of the Faraday-cup efficiency.

Figure 1 shows examples of the spectra of 19-MeV α particles taken at 90° and at 170° and accumulated for 7 h with a 250-nA beam of $^4He^{2+}$. The full width at half-maximum (FWHM) of the Pb groups is about 80 keV; the peaks in the spectra were identified by their kinematic variation with angle. Peaks from light contaminants in the target show the expected kinematic broadening. The inelastic group from the scattering to the ^{208}Pb 3^- state (2.614 MeV) is clearly identified and is well resolved in the spectra; the laboratory ratio of the inelastic-to-elastic scattering could be extracted with ~5% precision. The inelastic α groups have cross sections of 10–40 μb/sr and the inelastic-to-elastic ratios were $(0.6\text{–}1.0)\times10^{-4}$. In order to resolve the inelastic groups from the background high peak-to-valley ratios were essential; typical values for α's in this experiment (measured 3 MeV below the elastic peak) were $(4\text{–}6)\times10^4$:1, achieved by careful attention to collimator details. The background in this region was mainly due to slit scattering, and recent experience[11] suggests that it could perhaps be reduced still further. Dead-time corrections to the α data (<1%) were estimated from the known characteristics of the analyzers. Corrections were applied for the small differences in solid angles of different detectors. The geometrical solid angles were known to 0.1% and the same detectors and apertures were used for all the data taking.

The absolute inelastic cross section in the c.m. was obtained from the laboratory ratio R_{lab} of the inelastic-to-elastic yields and the actual c.m. elastic cross section by the expression

$$d\sigma(\theta')_{\text{inel}}/d\Omega = d\sigma(\theta)_{\text{el}}/d\Omega \times G'/G \times R_{\text{lab}},$$

where θ' and θ are the respective c.m. scattering angles. The ratio of the c.m.-to-lab cross sections is denoted by G for the elastic group and G' for the inelastic group. At 170° G is 1.039, but G'/G is only 1.0030. The deviation of the elastic scattering from Rutherford (Fig. 6 and Sec. IV) at 19 MeV was considerable and amounted to 12% at 170°. The value used for $d\sigma_{\text{el}}/d\Omega$ was the actual c.m. cross section as is discussed further in Sec. IV.

Traces of Si, S, and Cl contaminants were identified on the target, and at angles forward of 85° the elastic scattering groups from these elements were too close to the inelastic peak position to allow a reliable measurement. The percentage effect of the quadrupole moment on the inelastic angular distribution is largest at the backward angles, and this is where the data can be obtained with least interference from other groups.

The α peak marked ^{211}Po in the spectrum is of particular interest; it is attributed to the decay of 0.52-sec ^{211}Po by a 7.45-MeV α particle[12] and thus gives a direct measurement of the total cross section of the ^{208}Pb$(\alpha, n)^{211}$Po reaction. The total (α, n) cross section is 7.8±0.4 mb at 19 MeV, measured with the 144-μg/cm^2 target. The error quoted is statistical only, and the value with a 54-μg/cm^2 target was 10% less, indicating a possible loss of low-energy ^{211}Po ions before they decay. Recent measurements at this laboratory[13] have confirmed the ^{211}Po identification by determining the half-life and energy spectrum of the decay α's and finding very good agreement[12] with accepted values. The ^{211}Po peak has the same intensity in all detectors where it is not obscured. This reaction proceeds via compound nucleus formation and is the major cause of the deviation of the elastic scattering from the Rutherford value evident in Fig. 6. The (α, p) and (α, γ) reactions on ^{208}Pb have at most 1% of the (α, n) cross section, since

[11] F. Resmini, A. D. Bacher, D. J. Clark, E. A. McClatchie, and R. deSwiniarski, Nucl. Instr. Methods 74, 261 (1969).

[12] C. M. Lederer, J. M. Hollander, and I. Perlman, *Table of Isotopes* (John Wiley & Sons, Inc., New York, 1967), 6th ed.

[13] A. R. Barnett and J. S. Lilley, Contributions I.C.P.N.S. (Université de Montréal, Montreal, August 1969), p. 296.

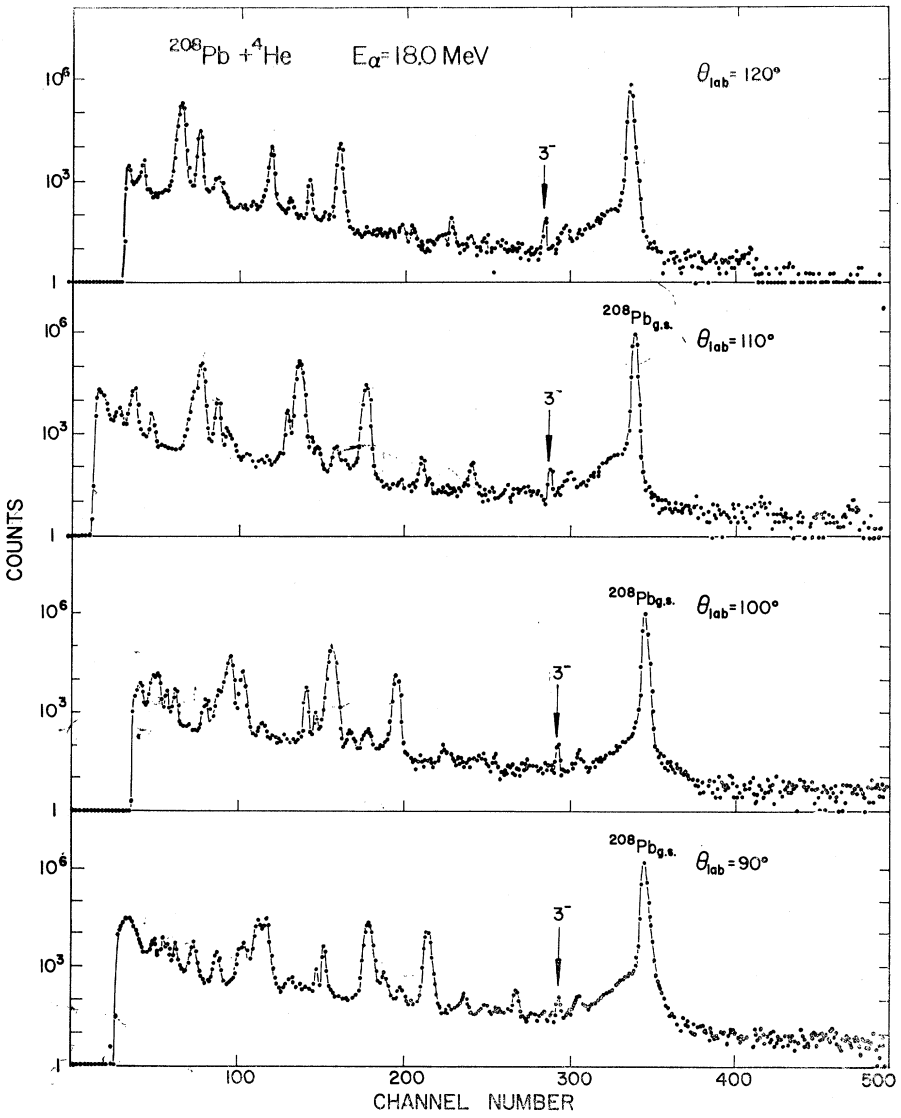

FIG. 2. Four of six simultaneous α spectra taken at 18-MeV bombarding energy on a 144-μg/cm^2 enriched ^{208}Pb target. The ratios of the 3^- inelastic peak to the elastic peak are about 5×10^{-4}, and the elastic group closely follows Rutherford scattering.

they did not appear in the spectrum, and other energetically allowed reactions have negligible Coulomb barrier penetration probabilities; the relative penetrability of $l=0$ protons to $l=0$ neutrons is 6×10^{-6} at 19 MeV. Table I summarizes the total α bombardments at the three energies.

The 18-MeV α data shown in Fig. 2 are four of six simultaneous spectra taken in 6 h with an average beam of 350 nA ^{4}He^{2+}. The broader peak between the inelastic 3^- peak and the ^{208}Pb elastic peak is seen in all the α spectra and is due to the ^{28}Si$(\alpha, \alpha_{1.78})^{28}Si^*(\gamma)^{28}$Si nuclear reaction of the elastic α's in the detector. The deexcitation γ ray escapes from the detector. The peak is shifted to a lower energy and broadened, probably because the high ion densities from the recoil Si result in imperfect charge collection (a pulse-height defect). The effect has been studied experimentally by Kraushaar *et al.*[14] for the case of 15.1-MeV protons, and they find quite good agreement between their data and theoretical predictions.

Figure 3 shows some of the 17.5-MeV α data taken in 5 h with a 1-μA ^{4}He^{2+} beam. Most of the contaminant peaks are identified, and also the expected position of the 2^+ state at 4.070 MeV in ^{208}Pb is indicated. No evidence was seen for the $E2$ Coulomb excitation of this state, consistent with the known $B(E2)$ value[15] of 0.3 e^2 b^2, for which the expected $\theta=\pi$ cross section is less than 0.07 of the $E3$ Coulomb excitation of the 3^- state. The pronounced tail extending to about 1 MeV below all the elastic peaks never amounted to more than 0.1% and

[14] J. J. Kraushaar, R. A. Ristinen, and R. Smythe, Phys. Letters **25B**, 13 (1967).
[15] C. F. Ziegler and G. A. Peterson, Phys. Rev. **165**, 1337 (1968).

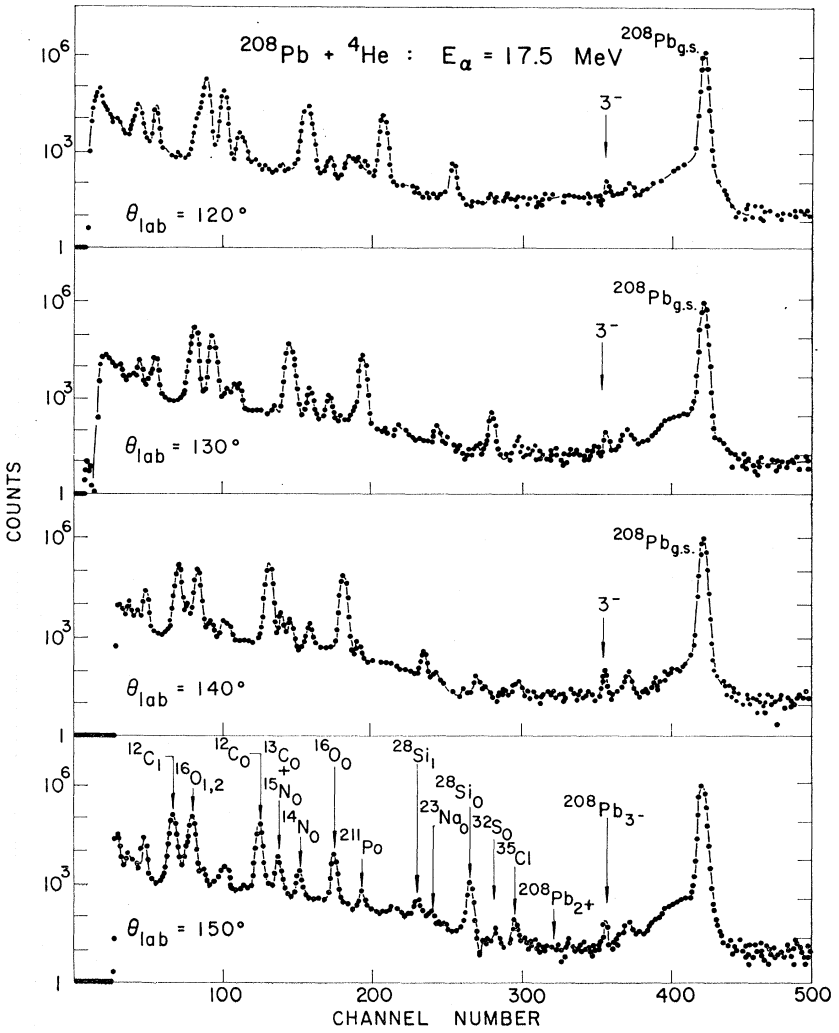

FIG. 3. Some of the 17.5-MeV α data, with target contaminant groups indicated and the expected ^{208}Pb 3^- and 2^+ (4.07-MeV) groups marked. Consistent with its known $B(E2)\uparrow$, the 2^+ 4.07-MeV quadrupole state in ^{208}Pb was not excited at our level of detection. The solid angles of all the detectors were equal. The broad peak above the 3^- inelastic group arises from the ^{28}Si(α, $\alpha\gamma$)^{28}Si reaction of incident α's on the detector, with the escape of the γ ray.

seems to be an individual detector phenomenon independent of count-rate, angle, and other variables. This tail does not affect the present measurement, but its presence sets a limit to the accuracy with which inelastic peaks with excitations <1 MeV can be measured with these detectors. Indeed, while spectra from a natural lead target (100 μg/cm^2) taken at 18 MeV showed the presence of the expected $E2$ Coulomb excited states at 570 and 897 keV in ^{207}Pb and at 803 keV in ^{206}Pb, the detector tail sharply limited the accuracy of that cross-section measurement. The natural lead spectra also showed a group at 2.6 MeV with about the same relative intensity as in the ^{208}Pb data. The peak is the unresolved group of states: 2.614 MeV in ^{208}Pb, 2.625 and 2.664 MeV in ^{207}Pb and 2.649 MeV in ^{206}Pb, all of which are excited with similar $B(E3)$ values.[15]

Examples of the ^{16}O spectra are shown in Fig. 4. These data were taken simultaneously in about 29 h using a 69.1-MeV $^{16}O^{6+}$ beam with an average intensity of 100 nA. Beams of 400 nA or greater severely worsened the resolution by melting parts of the target. The FWHM of the peaks is 300 keV. The inelastic cross sections are about 10 times larger than for the α case, while the elastic cross sections are about the same. The same collimators as for the α data were used, and they have equal solid angles (to within known corrections of $<0.3\%$). The relative elastic peak areas decrease with angle according to the Rutherford law, and Fig. 4 shows clearly the almost constant inelastic-to-elastic ratio of about 0.8×10^{-3}. The elastic G factor at 170° is 1.171, but the ratio G'/G again is only a small correction of 1.0035 at this angle. Dead-time corrections for the oxygen data were measured with a pulser which was triggered by the digital output pulses from the current integrator. The count-rate dead times amounted to 0.1%. As expected, the slit scattering for the oxygen was more pronounced, and at forward angles the increasing elastic tail and decreasing inelastic yield make the measurements less accurate. There was, naturally, no problem from light contaminants in these

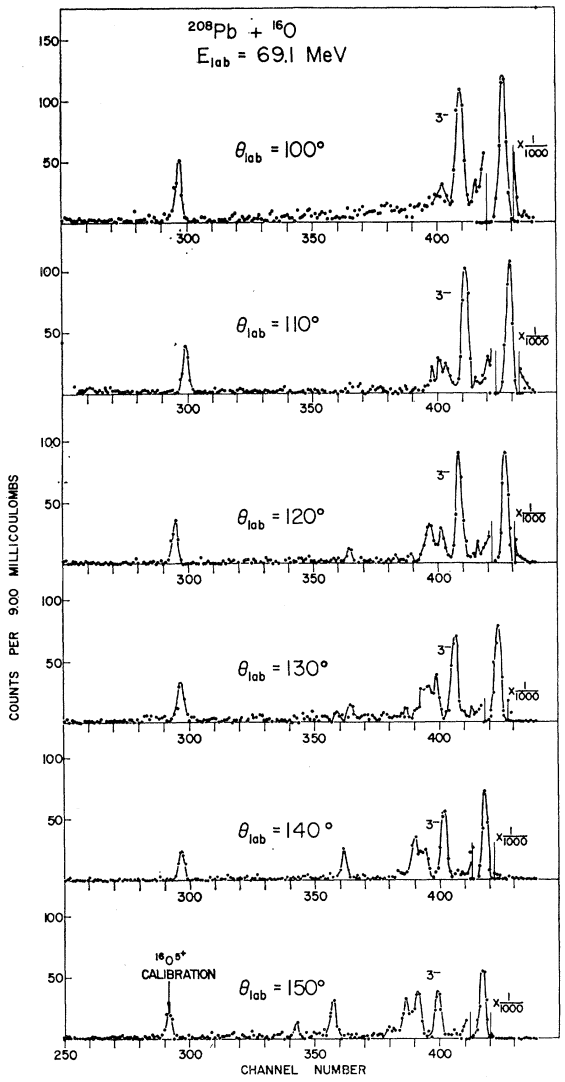

FIG. 4. An example of an oxygen run at 69.1 MeV on a 59-μg/cm^2 enriched ^{208}Pb target. All detectors have equal solid angles. The 3^- inelastic group is prominent with a ratio to the elastic group of $\sim 0.8\times 10^{-3}$. Also present at slightly lower energies are a number of groups attributed to nuclear tunnelling reactions. The calibration peak, of energy (25/36) E^{16}O, was obtained from a short bombardment with the 5^+ charge state of ^{16}O using the same analyzing magnet setting and a lower terminal voltage.

spectra. A calibration group (near channel 300) of energy 25/36 of the elastic oxygen energy was obtained from a short bombardment with the 5^+ charge state, using the same analyzing magnet setting and a lower terminal voltage of the Tandem. The peaks appearing between channels 340 and 400 were then identified as being due to various nucleon tunnelling reactions leaving the residual and outgoing nuclei in single-particle states. In the spectra (particularly at 160° and 170°) there is evidence for the following nucleon tunnelling reactions arising from ^{16}O+^{208}Pb: $^{17}O_{g.s.}+^{207}Pb_{g.s.}$, $^{17}O_{0.87}+^{207}Pb_{g.s.}$, and $^{17}O_{g.s.}+^{207}Pb_{0.897}$ (unresolved), $^{17}O_{g.s.}+^{207}Pb_{1.63}$, $^{15}N_{g.s.}+^{209}Bi_{0.892}$, and also $^{15}N_{g.s.}+^{209}Bi_{1.601}$. The nucleon tunnelling reactions peak at backward angles, as would be expected.[16] The $E2$ cross section to the 2^+ state of ^{208}Pb at 4.07 MeV has a predicted value of about 10% of the $E3$ cross section at 110°. There is evidence for it at channel 400; at other angles the $E2$ state tends to be obscured by nearby tunnelling peaks.

The elastic and inelastic angular distributions resulting from the α particle and the oxygen spectra are shown in Figs. 6, 7, and 9–12 and are discussed in Sec. IV.

III. THEORY

The theory of the Coulomb-excitation process has been extensively investigated by many authors and is presented in detail in the review article of Alder *et al.*[4] which also appears (with corrections) in the useful reprint selection on Coulomb excitation by Alder and Winther.[2] Excitations by nuclear interactions between the target and the bombarding ion are specifically excluded from the theory, which then predicts the probability of excitation (P) of nuclear levels caused by the time-dependent electromagnetic interaction. The absolute cross section for the excitation is obtained on the assumption that the sum of the elastic and Coulomb-excited inelastic cross sections follows the Rutherford law, i.e.,

$$d\sigma = P d\sigma_{\text{Ruth.}} \tag{1}$$

The electric multipole operators causing the nuclear transition are defined[4] as

$$\mathbf{M}(E\lambda, \mu) = \int r^\lambda Y_{\lambda\mu}(\theta, \phi)\rho(\mathbf{r})d\tau,$$

and the unknown quantities in the theory are the reduced transition matrix elements of these operators (in various multipole orders) between the levels; it is this nuclear information which is obtained by comparison with experiment. For example, the reduced matrix element between the ground state and the excited state under consideration, $B(E\lambda)=B(E\lambda)\uparrow$, defined as

$$B(E\lambda, I_i \rightarrow I_f) = (2I_i+1)^{-1} |\langle I_i || \mathbf{M}(E\lambda, \mu) || I_f\rangle|^2,$$

occurs as a scale factor which, in principle, could be determined by a single measurement of the ratio of the inelastic to elastic cross section at one angle. It is, however, essential to check experimentally that the assumptions of the theory hold, and without such test a single point could give an unreliable result.

The influence of the static nuclear multipole moments in the Coulomb-excitation process is in general called the reorientation effect; considerable attention[1–3] has been concentrated on the deviations to be expected from the first-order theory from the effect of the static quadrupole moment Q of the first excited state. A number of experimental attempts (summarized in the

[16] G. Breit, Phys. Rev. 135, B1323 (1964), and references therein.

TABLE II. Calculated parameters for the various experimental conditions. The symbols are defined in Sec. III. The energy is quoted at a point halfway through the target.

Energy (MeV)	Ion	η_i	ξ_{if}	v_i/c	v_f/v_i	a_{if} (F)	$d\sigma_B^{(1)}/d\sigma_A^{(1)}$ [a]
19.0	$^4He^{2+}$	11.852	0.930	0.1010	0.9272	6.831	0.9818
18.0	$^4He^{2+}$	12.177	1.015	0.0982	0.9230	7.243	0.9831
17.5	$^4He^{2+}$	12.350	1.063	0.0969	0.9207	7.469	0.9837
69.02	$^{16}O^{6+}$	49.725	1.046	0.0963	0.9794	7.524	0.9989

[a] This value is the ratio of $d\sigma^{(1)}$ calculated using the Biedenharn-Brussard symmetrization expression to $d\sigma^{(1)}$ calculated from the Alder *et al.* expression, as discussed at the end of Sec. III.

review of de Boer and Eichler,[1] and also, more recently, in Refs. 17–19) have been made to measure this effect and, by isolating it from competing second-order processes, to determine Q for excited 2^+ states in both light- and medium-mass nuclei. All these experiments have thus considered the reorientation effect following $E2$ Coulomb excitation. They have used a variety of incident ions (^{4}He to ^{32}S) and bombarding energies, and the direct inelastic scattering technique as well as various γ-ray techniques, e.g., measuring de-excitation γ rays in coincidence with back-scattered heavy ions.[5] In the case where the $E2$ inelastic cross sections are large, and multiple Coulomb excitation takes place, the $E2$ computer code of Winther and de Boer[20] has often been used. Conversely, when the excitation probabilities are small, and the semiclassical theory is valid, the perturbation theory results of Alder *et al.*[4] can be used to calculate the absolute excitation probability.

The measurement of the reorientation effect following $E3$ Coulomb excitation reported in this paper was interpreted using the second-order perturbation theory results of Alder *et al.*[4] The probability of excitation in the α experiments is 10^{-4}, and in the ^{16}O case it is 10^{-3}; as we discuss later it does not follow that the higher-order terms in a perturbation calculation of the cross section will be small relative to the first-order term. The observed cross section for inelastic scattering, $d\sigma$, is written

$$d\sigma = d\sigma^{(1)} + d\sigma^{(1,2)} + d\sigma^{(2)} \qquad (2)$$

as in Eq. (II D 11) of Ref. 4. Here, $d\sigma^{(1)}$ is the first-order excitation cross section, $d\sigma^{(1,2)}$ is the cross product between the first- and second-order transitions, and $d\sigma^{(2)}$ is the second-order cross section. The semiclassical theory is applicable when the dimensions of the orbit are much larger than the relative Compton wavelength, so that wave packets can be constructed which follow classical hyperbolic orbits. The ratio of the Coulomb length a to the Compton wavelength of relative motion is defined as the Sommerfeld parameter η:

$$\eta = a/\lambda\!\!\!^{-} = (Z_1 Z_2 e^2/m_0 v^2)/(\hbar/m_0 v),$$

where m_0 is the reduced mass of the bombarding ion. The values of η_i for our experimental conditions are given in Table II along with other relevant quantities. The other parameters in the theory are defined in a symmetrized manner[4] as follows:

$$a_{if} = Z_1 Z_2 e^2/m_0 v_i v_f, \qquad (3)$$

$$\eta_i = Z_1 Z_2 e^2/\hbar v_i, \qquad (4)$$

$$\xi_{if} = \eta_f - \eta_i, \qquad (5)$$

in the usual attempt to define a mean classical orbit having an excitation probability along it which would closely approximate the results of using a full quantal calculation.

The general second-order perturbation-theory result for the various terms in (2) is given in Ref. 4: the expression for $d\sigma^{(1)}$ in Eq. (II A 28), for $d\sigma^{(1,2)}$ in Eq. (II D 12), and for $d\sigma^{(2)}$ in Eq. (II D 13). The functions $\alpha_{k\kappa}(\lambda_1\lambda_2\xi_1\xi_2, \theta)$ and $\beta_{k\kappa}(\lambda_1\lambda_2\xi_1\xi_2, \theta)$ are defined in terms of the classical orbital integrals $I_{\lambda\mu}(\theta, \xi)$ according to Eqs. (II D 9) and (II D 10) of Ref. 4. The electromagnetic transitions induced by the Coulomb field of the projectile take place from the initial state i through an intermediate state z to the final state f, with the ξ parameter of the two transitions being written $\xi_{iz} = \eta_z - \eta_i \equiv \xi_1$ and $\xi_{zf} = \eta_f - \eta_z \equiv \xi_2$. The summations in the equations cited are to be taken over all possible second-order paths leading to the final state. Besides the reorientation effect, for which $z=f$, the most important contributions to $d\sigma^{(1,2)}$ may be expected to be (a) the $E2, E1$ path $0^+ \rightarrow 2^+ \rightarrow 3^-$ via the one-phonon quadrupole vibration in ^{208}Pb [this is a state of 4.07 MeV which has the large $B(E2)$ value[15] of $0.3e^2$ b^2 or nine single-particle units (s.p.u.)], and (b) the $E1, E2$ path $0^+ \rightarrow 1^- \rightarrow 3^-$ via the giant dipole resonance, which is situated in ^{208}Pb at about 15 MeV.[21] We evaluated $d\sigma^{(1,2)}$ for path (a), using the known $B(E2)\uparrow$ and assuming that the $B(E1)\downarrow$ for the $2^+ \rightarrow 3^-$ transition was 10^{-3} s.p.u.[22]

[17] J. J. Simpson, U. Smilansky, and J. P. Wurm, Phys. Letters **27B**, 633 (1968); **28B**, 422(E) (1969); J. X. Saladin, J. E. Glenn, and R. J. Pryor, Phys. Rev. (to be published).

[18] A. Bamberger, P. G. Bizzeti, and B. Povh, Phys. Rev. Letters **21**, 1599 (1968); O. Häusser, B. W. Hooton, D. Pelte, T. K. Alexander, and H. C. Evans, *ibid.* **22**, 359 (1969); J. R. Kerns, J. X. Saladin, R. J. Pryor, and S. A. Lane, Bull. Am. Phys. Soc. **14**, 122 (1969); **14**, 123 (1969); G. Engler, *ibid.* **14**, 122 (1969).

[19] D. Cline, H. S. Gertzman, H. E. Gove, P. M. S. Lesser, and J. J. Schwartz, Nucl. Phys. **A133**, 445 (1969).

[20] A. Winther and J. de Boer, in *Coulomb Excitation*, edited by K. Alder and A. Winther (Academic Press Inc., New York, 1966), p. 303.

[21] E. G. Fuller and Evans Hayward, in *Nuclear Reactions*, edited by P. M. Endt and P. B. Smith (North-Holland Publishing Co., Amsterdam, 1962), Chap. III, p. 113.

[22] The single-particle unit is defined in Eq. (13).

TABLE III. Theoretical predictions using the symmetrized second-order perturbation expressions of Eqs. (6)–(8) for the absolute cross sections for α's at 18 MeV and for oxygen at 69.02 MeV. The basic parameters $B(E3)=0.58e^2$ b^3 and $Q=1.0$ b were used in the calculations.

Beam	Angle	$d\sigma^{(1)}$ (μb/sr)	$d\sigma^{(1,2)}$ (μb/sr)	$d\sigma^{(2)}$ (μb/sr)	$d\sigma^{(1)}-d\sigma^{(1,2)}$ (μb/sr)	$d\sigma_{\text{Ruth}}$ (mb/sr)	$10^4\, d\sigma^{(1)}/d\sigma_{\text{Ruth}}$
$^{16}O^{6+}$	π	148.49	34.33	5.08	114.16	135.75	10.94
	$\frac{1}{2}\pi$	289.53	27.69	2.29	261.84	543.00	5.33
$^4He^{2+}$	π	11.81	0.73	0.029	11.08	111.75	1.06
(18 MeV)	$\frac{1}{2}\pi$	22.53	0.57	0.013	21.96	446.99	0.50

It is unlikely that the transition is so strong, yet the contribution to $d\sigma^{(1,2)}$ from (a) is less than 3% of that provided by the reorientation effect with a quadrupole moment of 1 b. In the case of path (b) we simulated the effect of the giant dipole resonance by a single state at 15 MeV with a $B(E1)\uparrow$ from the ground state of 10 s.p.u. and a $B(E2)\downarrow$ for the $1^-\rightarrow 3^-$ transition of 0.1 s.p.u. (again, improbably large); the result was similar to that for path (a), and hence more detailed considerations[1] are not necessary. We thus believe that in the case of ^{208}Pb no second-order paths involving other levels are affecting the Coulomb-excitation cross section. The "$M1$ reorientation effect," i.e., second-order paths involving magnetic dipole transitions between the substates of the 3^- levels, is difficult to estimate: It has been shown[1] that in the case of quadrupole Coulomb excitation of 2^+ levels in even-even nuclei the effect is negligible compared with the $E2$ reorientation. We assume that this is also true in the case of octupole Coulomb excitation; and hence the general theoretical expressions given in Ref. 4 can be specialized to the situation where only one final 3^- level and only the quadrupole reorientation effect are important. The summations over intermediate states simplify greatly and the results are

$$d\sigma^{(1)}=(4\pi^2/7^3)\,(Z_1e/\hbar v_i)^2 a_{if}^{-4}\sin^{-4}(\tfrac{1}{2}\theta)\,d\Omega\times B(E3)\times\sum_\mu Y_{3\mu}(\tfrac{1}{2}\pi,0)I_{3\mu}{}^2(\theta,\xi),\quad(6)$$

$$d\sigma^{(1,2)}=\frac{16\pi^3}{5\times 7^3}\left(\frac{21}{4\pi}\right)^{1/2}\left(\frac{Z_1e}{\hbar v_i}\right)^3\left(\frac{v_i}{v_f}\right)^{1/2}a_{if}^{-6}\sin^{-4}(\tfrac{1}{2}\theta)\,d\Omega\times B(E3)\times eQ\times\sum_\mu Y_{3\mu}(\tfrac{1}{2}\pi,0)I_{3\mu}(\theta,\xi)\beta_{3-\mu}(32\xi0,\theta),\quad(7)$$

and

$$d\sigma^{(2)}=\frac{12\pi^3}{5^2\times 7^3}\left(\frac{Z_1e}{\hbar v_i}\right)^4\left(\frac{v_i}{v_f}\right)a_{if}^{-8}\sin^{-4}(\tfrac{1}{2}\theta)\,d\Omega\times B(E3)\times e^2Q^2\times\sum_\mu[\alpha_{3\mu}{}^2(32\xi0,\theta)+\beta_{3\mu}{}^2(32\xi0,\theta)],\quad(8)$$

where the static quadrupole moment Q, of a state with spin I is defined[4] as

$$eQ=(16\pi/5)^{1/2}\langle I\,||\,\mathbf{M}(E2)\,||\,I\rangle\times[I(2I-1)/(2I+1)(I+1)(2I+3)]^{1/2}.\quad(9)$$

The functions $\alpha_{k\kappa}$ and $\beta_{k\kappa}$ become

$$\alpha_{k\kappa}(32\xi0,\theta)=\sum_{\mu_1\mu_2}\begin{pmatrix}3&2&3\\ \mu_1&\mu_2&\kappa\end{pmatrix}Y_{3\mu_1}(\tfrac{1}{2}\pi,0)\,Y_{2\mu_2}(\tfrac{1}{2}\pi,0)\times I_{3\mu_1}(\theta,\xi)I_{2\mu_2}(\theta,0),$$

$$\beta_{k\kappa}(32\xi0,\theta)=\sum_{\mu_1\mu_2}\begin{pmatrix}3&2&3\\ \mu_1&\mu_2&\kappa\end{pmatrix}Y_{3\mu_1}(\tfrac{1}{2}\pi,0)\,Y_{2\mu_2}(\tfrac{1}{2}\pi,0)\times\frac{1}{\pi}\,\mathcal{P}\int_{-\infty}^{\infty}\frac{dx}{x}\,I_{3\mu_1}(\theta,\xi+x)I_{2\mu_2}(\theta,-x),$$

with $\xi=\xi_{if}$. These functions and Eqs. (6)–(8) were evaluated on the CDC 3100 computer at the Williams Laboratory. The orbital integrals required, $I_{3\mu}(\theta,\xi)$ and $I_{2\mu}(\theta,\xi)$, are tabulated by Alder and Winther[23] for a range of values of ξ at 10° intervals; they were interpolated to the appropriate ξ value by the Lagrange method using the more slowly varying function $\ln I_{\lambda\mu}(\xi)$. The 1963 values of the Atomic Constants were used[24] in the calculations.

The sensitivity of the theoretical predictions of the cross section to the higher-order terms $d\sigma^{(1,2)}$ and $d\sigma^{(2)}$ is shown in Fig. 5 and in Table III. The value of the cross section $d\sigma^{(1)}+d\sigma^{(1,2)}$ is plotted in Fig. 5 for α's and for ^{16}O, with $B(E3)=0.58e^2$ b^3, both for $Q=0$ (i.e., $d\sigma^{(1)}$ alone) and for $Q=-1.3$ b. The oxygen data are seen to be rather sensitive to Q, and $d\sigma^{(1,2)}/d\sigma^{(1)}=0.23$ for $Q=1$ b at $\theta=\pi$; for α's the value is 0.06 at $\theta=\pi$, and the sensitivity to Q is much less. Nevertheless, we will show in Sec. V that *both* the α data and the oxygen data are essential in limiting the values of $B(E3)$ and Q that simultaneously fit all the experimental results.

It is at first sight surprising that the perturbation expressions, Eqs. (6)–(8) that correctly predict an excitation probability of 10^{-3} for $d\sigma^{(1)}(^{16}O)$ should also predict such a large contribution from the higher orders. A measure of the perturbation expansion parameter is

[23] K. Alder and A. Winther, Kgl. Danske Videnskab. Selskab, Mat.-Fys. Medd. **31**, No. 1 (1956).

[24] It seems common practice in current work to use the original numerical constants given by Alder *et al.*[4] based on the proton-mass scale, e.g., the number 12.65 in the numerical expression for ξ. Using the ^{12}C-mass scale and the 1963 Atomic constants, we find this constant $(2\sqrt{2}/\alpha u^{1/2})$ to be 12.699 MeV$^{-1/2}$, where α is the fine-structure constant and u is the atomic mass unit in MeV. However, even though a significant change in ξ and in $I_{\lambda\mu}{}^2(\xi)$ results, the final absolute theoretical cross sections differ by less than 0.05% in the $E3$ case.

the value of the function $F_{if}^{(3)}(\pi, \xi)$, defined[2,25] to be the square root of the excitation probability for backward scattering: In general we define[26] an amplitude parameter for any angle θ as

$$F_{if}^{(\lambda)}(\theta, \xi) = [P_{if}^{(\lambda)}(\theta, \xi)]^{1/2}. \quad (10)$$

For the $E3$ experiment we have the small expansion parameter ($\xi = \xi' \sim 1.0$)

$$F_{if}^{(3)}(\pi, \xi') = 0.01 \quad \text{for the } \alpha \text{ experiments}$$
$$= 0.03 \quad \text{for the } ^{16}\text{O experiment.}$$

This parameter, however, contains both the *intrinsic* strength of the coupling between the states i, f by the interactions with the electromagnetic field of the projectile, and various ξ-dependent terms, having the approximate form $e^{-2\pi\xi}$. Thus the intrinsic coupling strength $\chi_{if}^{(\lambda)}$ of the $i \rightarrow f$ transition is defined[2,25] to be the value of $F_{if}^{(\lambda)}(\theta, \xi)$ with both $\theta = \pi$ and $\xi = 0$ (the zero energy-loss case). Consequently, the general symmetrized intrinsic strength parameter, using Eq. (10), becomes

$$\chi_{if}^{(\lambda)} \equiv F_{if}^{(\lambda)}(\theta = \pi, \xi = 0)$$
$$= 4\pi^{1/2} \frac{(\lambda-1)!}{(2\lambda-1)!!} \frac{Z_1 e}{\hbar v_{if}} \frac{\langle I_f \| \mathbf{M}(E\lambda) \| I_f \rangle}{a_{if}^{\lambda}(2I_i+1)}, \quad (11)$$

where the symmetrized velocity $v_{if} = (v_i v_f)^{1/2}$. The parameter $\chi_{if}^{(\lambda)}$ was introduced by Alder and Winther[25] in their discussion of multiple Coulomb excitation. The $E3$ intrinsic strength $\chi_{if}^{(3)} = 0.14$ and the quadrupole interaction intrinsic strength $\chi_{ff}^{(2)} = 0.31$. While the $E3$ and $E2$ *intrinsic* strengths are comparable, the *effective* strengths[26] in the perturbation expansion are given by $F_{if}^{(3)}(\pi, \xi')$ and $F_{ff}^{(2)}(\pi, 0)$, and these differ in the ratio 1:10.

The $d\sigma^{(2)}$ term for ^{16}O is only 3% of $d\sigma^{(1)}$ at $\theta = \pi$ for $Q = 1$ b, and Fig. 5 shows that it is even less important at other angles. There are many higher-order $d\sigma^{(1,3)}$ paths by which terms of the order of $d\sigma^{(2)}$ can arise and which may have either sign relative to $d\sigma^{(2)}$. Masso and Lin[27] have evaluated some $d\sigma^{(1,3)}$ terms for $E2$ Coulomb excitation and show that one term largely cancels the $d\sigma^{(2)}$ term over a range of ξ values. No third-order theory exists for $E3$ Coulomb excitation, and the only second-order (unsymmetrized) calculation known to us is that of Beder[28] for the case of the $E3$ excitation of the $\frac{5}{2}^-$ 1.35-MeV state in ^{19}F. In the absence of specific estimates of $d\sigma^{(1,3)}$ terms, we decided to neglect the $d\sigma^{(2)}$ term in evaluating the theoretical cross section, and we fitted the data to the expression

$$d\sigma = d\sigma^{(1)} + d\sigma^{(1,2)}$$
$$= B(E3) A(\theta)[1 + QB(\theta)], \quad (12)$$

leaving two parameters to be determined: $B(E3)$ and Q. It should be noted that were Q to have a "rotational value" of about -5 b, then $d\sigma^{(2)}$ would be comparable with $d\sigma^{(1,2)}$ and with $d\sigma^{(1)}$, so that the perturbation treatment would not be applicable to all. In the ^{208}Pb case, with $Q = -1.3$ b, the perturbation expansion is reasonably adequate.

The theoretical predictions and the parameters involved were symmetrized according to the method suggested by Alder *et al.*[4] as given in Eqs. (3)–(5). This leads to the factors

$$(Z_1 e/\hbar v_i)^3 (v_i/v_f)^{1/2} \quad \text{and} \quad (Z_1 e/\hbar v_i)^4 (v_i/v_f)$$

(as well as terms containing the symmetrized param-

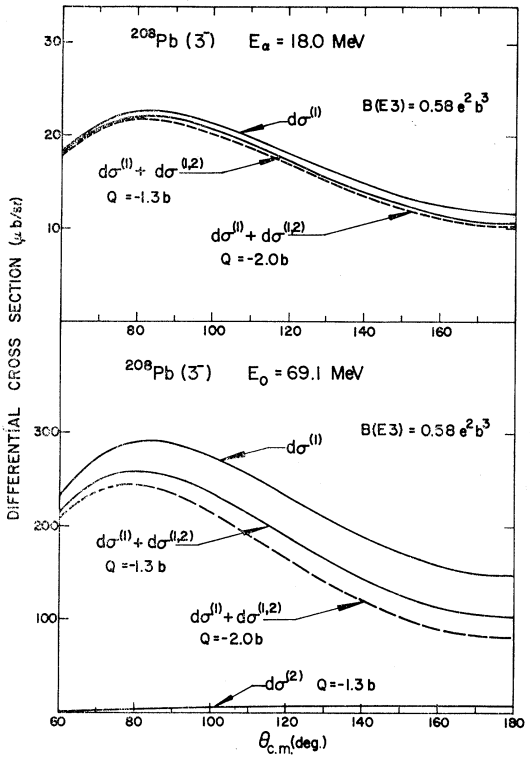

FIG. 5. Sensitivity of the predicted α and oxygen angular distributions to the value of the quadrupole moment of the 3^- state. For α's, $d\sigma^{(2)}$ was negligible, and for oxygen it was small, as indicated. The final data, for reasons discussed in the text, were fitted to an expression of the form $d\sigma = d\sigma^{(1)} + d\sigma^{(1,2)}$.

[25] K. Alder and A. Winther, Kgl. Danske Videnskab. Selskab, Mat.-Fys. Medd. **32**, No. 8 (1960), reprinted in Ref. 2.

[26] Alder and Winther (Ref. 25) introduced the function $F_{if}^{(\lambda)}(\theta, \xi)$—which is called $\chi_{if}^{(\lambda)}(\theta, \xi)$ in their Eq. (2.10)—to be the measure of the perturbation expansion parameter. We have altered the notation to avoid confusion between the *function* $\chi_{if}^{(\lambda)}(\theta, \xi)$ and the strength *parameter* $\chi_{if}^{(\lambda)}$ [Eq. (11) above and Eq. (2.11) of Ref. 25], which measures the intrinsic strength of the $E\lambda$ transition in the nucleus (Ref. 1). However, it is the value of the function $F_{if}^{(\lambda)}(\theta, \xi)$ which determines the applicability of perturbation theory (Ref. 25) rather than the value of the strength parameter $\chi_{if}^{(\lambda)}$ alone (although the condition $\chi_{if}^{(\lambda)} \ll 1$ is certainly a sufficient one). The function $F_{if}^{(\lambda)}(\theta, \xi)$ is the product of $\chi_{if}^{(\lambda)}$ and ξ-dependent orbital integrals.

[27] J. F. Masso and D. L. Lin, Phys. Rev. **140**, B1182 (1965).

[28] D. Beder, Phys. Letters **3**, 206 (1963).

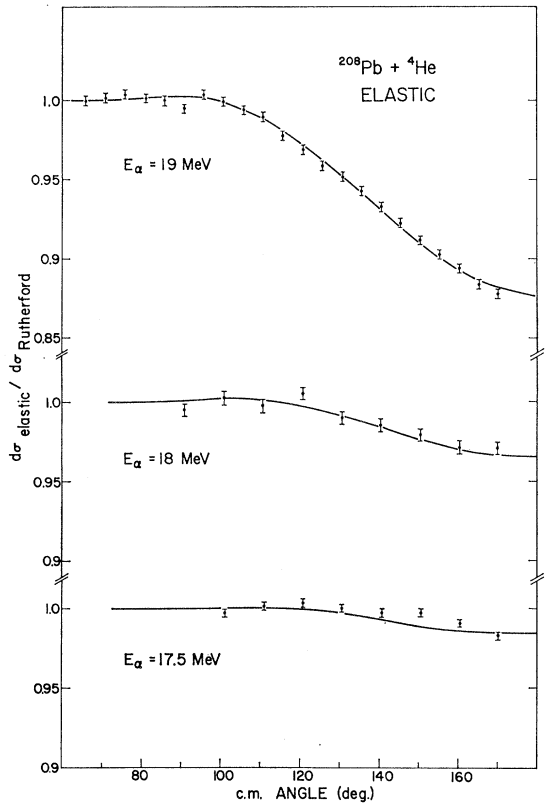

FIG. 6. Elastic α angular distributions at 19, 18, and 17.5 MeV plotted as a ratio to the Rutherford value. The target thickness was calculated by assuming Rutherford scattering at the forward angles. Statistical and systematic errors are $\lesssim$0.5%. The solid curves are optical-model fits to the data with the only variable being the depth of the imaginary part of the potential, W_D. The form used was

$$V(r) = -V_R f(r,r_0,a) + V_{\text{Coul}},$$
$$W(r) = W_D 4a'(d/dr) f(r,r_0',a'),$$

where $f(r,r_0,a) = \{1+\exp[(r-r_0A^{1/3})/a]\}^{-1}$ and V_{Coul} is the potential of a uniformly charged sphere of radius $r_cA^{1/3}$. The fixed parameters were $V_R = 225$ MeV, $r_0 = 1.17$ F, $a = 0.70$ F, $r_0' = 1.30$ F, $a' = 0.70$ F, and $r_c = 1.25$ F; W_D had the values 18, 10, and 6 MeV and the bombarding energies of 19, 18, and 1.75 MeV, respectively.

eters a_{if} and ξ_{if}) appearing in Eqs. (5) and (6), respectively, for $d\sigma^{(1,2)}$ and $d\sigma^{(2)}$. Values of (v_f/v_i) are given in Table II. It is assumed in Ref. 28 that for heavy-ion Coulomb excitation with large values of η the differences between the symmetrized and unsymmetrized semiclassical calculations is very small, but that is not the case. For our example of ^{16}O+^{208}Pb with $\eta = 50$, the difference between the first-order calculations is 25%, i.e., $d\sigma_{\text{unsym}}{}^{(1)}/d\sigma_{\text{sym}}{}^{(1)} = 1.25$ at $\theta = \pi$. The two effects of the symmetrization procedure are an increase[29] of ξ and an increase[29] of a, and both effects decrease the cross section. For the case of 18-MeV α particles on ^{208}Pb with $\eta = 12$, we have

$$d\sigma_{\text{unsym}}{}^{(1)}/d\sigma_{\text{sym}}{}^{(1)} = 2.20$$

at $\theta = \pi$, while[28] for 30-MeV ^{19}F on ^{28}Si ($\eta = 16$) the ratio is 1.32.

The symmetrization procedure is to some extent *ad hoc*, and the question of the accuracy with which the symmetrized semiclassical cross section approaches the result of the quantal calculation has been investigated by many authors[1,2,4,10,30] with the emphasis heavily on the $E2$ case. Smilansky[10] has calculated quantal effects in two-channel multiple Coulomb excitation of 2^+ states and finds that deviations from the symmetrized semiclassical calculation become important for small η, small ξ, and for light nuclei. We assume that these general conclusions apply to $E3$ Coulomb excitation, and from the results discussed in his paper we expect that quantal corrections should be very small. Biedenharn and Brussard[30] discuss the symmetrization procedure in detail and suggest an alternative method to the usual (Alder *et al.*[4]) replacement of v by $(v_iv_f)^{1/2}$, or, equivalently, η by η_A, where

$$\eta_A = (\eta_i\eta_f)^{1/2}.$$

They replace η by η_B, where

$$\eta_B = \{2(\eta_i^2+1)(\eta_f^2+1)/[(\eta_i^2+1)^{1/2}+(\eta_f^2+1)^{1/2}]\}^{1/3}$$

while still retaining the definition $\xi_{if} = \eta_f - \eta_i$. For large values of $\eta_i \sim \eta_f$, the expression $\eta_B \sim (\eta_i^2+1)^{1/2}$. We evaluated the ratio of cross sections using the two procedures, i.e.,

$$d\sigma_B{}^{(1)}/d\sigma_A{}^{(1)} = \eta_A{}^6/\eta_B{}^6, \qquad \text{for all } \theta, \xi$$

and found that for ^{16}O the change is a 0.1% effect, while for ^{4}He it is a 2% effect (Table II), well within our experimental accuracy.

The ratios v_i/c and v_f/c are $\sim$0.1, so that relativistic effects[4] might be expected to be of the order of 1 or 2% of $d\sigma^{(1)}$.

IV. ANALYSIS

The differential cross sections for the elastic scattering of α particles off ^{208}Pb at 19, 18, and 17.5 MeV are given in Fig. 6, and the 69.1-MeV ^{16}O elastic scattering results in Fig. 11. These are plotted as a ratio to the Rutherford cross section and were obtained by measuring the angular distribution of the elastic group, using the six- or eight-detector array and a monitor detector. Over the range of angles where the distribution followed Rutherford scattering we assumed that the cross section was given by the Rutherford law; the absolute cross sections for the inelastic groups were then obtained directly from the ratios of the counts in the inelastic and elastic peaks, and the absolute elastic cross section. The corrections for the ratios of the inelastic to elastic

[29] In terms of the ratio $\zeta = \Delta E/E_{\text{c.m.}}$, where ΔE is the excitation energy, we have $\xi_{if} = \eta_i(v_i/v_f - 1) = \xi_{\text{unsym}}[1+\frac{3}{4}\zeta+\frac{5}{8}\zeta^2+(35/32)\zeta^3+\cdots]$ and $a_{if} = a_{\text{unsym}}v_i/v_f = a_{\text{unsym}}(1+\frac{1}{2}\zeta+\frac{3}{8}\zeta^2+\frac{5}{16}\zeta^3+\cdots)$.

[30] L. C. Biedenharn and P. J. Brussard, *Coulomb Excitation* (Clarendon Press, Oxford, 1965), Chap. III.

solid-angle conversion factors are very small (Sec. II), and the c.m. angles of observation of the two groups also are very slightly different. The inelastic scattering angular distributions are plotted in Figs. 7, 9, 10, and 12. The full lines in the figures are theoretical predictions of $d\sigma(\theta)/d\Omega$ for the best-fit parameters, using Eq. (12). All the data sets (except the 19-MeV α data) were analyzed simultaneously, and so the lines are not the best fit to the individual data sets of each of the figures.

A. 19-MeV α Data

At 19 MeV there is a large deviation from pure Coulomb scattering (12% at 170°) because of compound-nucleus formation: Direct processes have negligible cross sections compared with the compound-nucleus cross section $d\sigma_{cn}$, and the inelastic Coulomb excitation is only 10^{-4} of the elastic scattering. The compound nucleus ^{212}Po will decay almost entirely by neutron emission, and the subsequent α decay of the residual nucleus ^{211}Po leads to the 7.45-MeV α groups in the spectra of Figs. 1–3. The full lines through the data points of Fig. 6 are optical-model predictions for the parameters given in the caption. All the parameters in the fits were held constant at the three energies except the depth of the imaginary potential, which was reduced at the lower energies. The predicted total reaction cross section agrees with the measured (α, n) total cross section to within a factor of 2, and doubtless this agreement could be improved by further parameter variation.

The differential cross section for the inelastic group arising from the excitation of the 3^- level is shown in Fig. 7, together with the prediction based on pure Coulomb excitation of the level. We have used the final parameters $B(E3)=0.58e^2$ b^3 and $Q=-1.3$ b, but

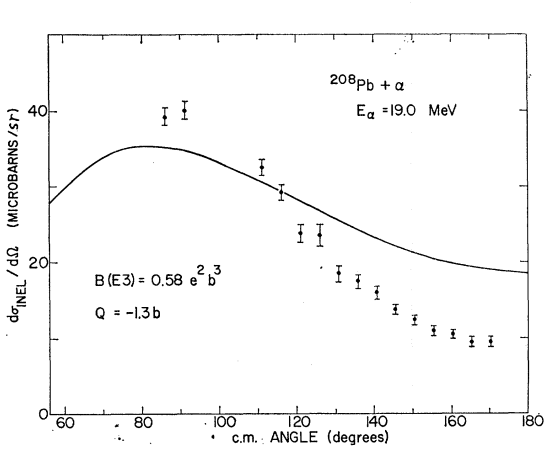

FIG. 7. Absolute inelastic angular distribution of the scattering cross section to the 3^- state of ^{208}Pb at 19-MeV incident α energy obtained from the inelastic-to-elastic ratios (see Fig. 1) and the absolute elastic cross section derived from Fig. 6 (see text). The curve is calculated with the best-fit parameters that fit the lower α energy data and the oxygen data. Strong interference from direct nuclear excitation is present and distorts the distribution (Sec. IV).

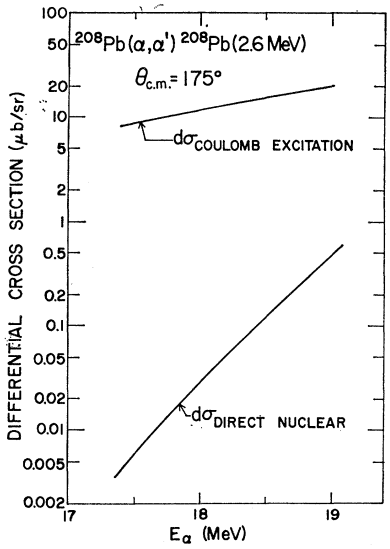

FIG. 8. Comparison of the $E3$ Coulomb excitation first-order cross section, Eq. (6), with the direct nuclear cross section as a function of incident α energy. The direct nuclear curve was calculated using a distorted-wave coupled-channels code, as described in Sec. IV A, with a deformability parameter of $\beta_3=0.11$. The optical-model parameters at 18 MeV, in the form given in the caption to Fig. 5, were $V_R=200$ MeV, $r_0=1.22$ F, $a=0.70$ F, $W_D=17$ MeV, $r_0'=1.30$ F, $a'=0.51$ F, and $r_c=1.25$ F. The rapid energy variation of $d\sigma_{dn}$, rather than its precise numerical value, is the important point.

since the effect of Q is less than 6%, the curve is close to the first-order prediction alone. The value of $B(E3)$ is known to lie in the range 0.3–0.8 e^2 b^3 from a number of earlier experiments (Sec. V), and this fixes the *total* inelastic cross section prediction: The *total* inelastic cross section, estimated from Fig. 7, is within these limits, and we can be confident that most of the total cross section is due to Coulomb excitation. The differential cross section of Fig. 7, however, shows a marked deviation[31] from the Coulomb-excitation theory which we attribute to an interference between a (small) amplitude for the direct excitation of the 3^- level via the tail of the nuclear potential and the amplitude for Coulomb excitation.

The curves in Fig. 8 are estimates of these effects for $\theta=175°$ as a function of α particle energy E_α. The curve labeled $d\sigma_{ce}^{(1)}$ is the first-order Coulomb-excitation differential cross section, calculated for $B(E3)=0.58e^2$ b^3. That labeled $d\sigma_{dn}$ gives the variation of the differential

[31] It is instructive to note that the data of Fig. 7 can be fitted quite well with an expression of the form $d\sigma=A(\theta)B(E3)[1+B(\theta)Q]$, i.e., Eq. (12), with a large negative Q of about 9 b [and a $B(E3)$ of $0.8e^2$ b^3]. (Of course, for such an unreasonably large quadrupole moment, considerably exceeding the "rotational value", second- and higher-order terms cannot be neglected, and the perturbation expansion is no longer valid.) Nevertheless, this observation does emphasize that measurements made at too high a bombarding energy, when effects other than Coulomb excitation are present, can give totally misleading information. The same peculiarity has been noted in the fitting of differential cross sections for the inelastic scattering to the 2^+ states of even-even nuclei (Ref. 19).

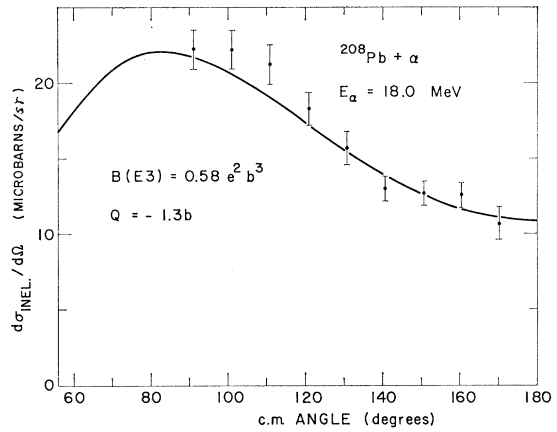

FIG. 9. Absolute angular distribution of the inelastic α scattering cross section to the 3^- ^{208}Pb state at 18-MeV incident energy. The curve is a fit to the data of Figs. 9, 10, and 12 simultaneously and is not the best fit to individual distributions.

cross section for direct nuclear inelastic scattering, calculated by using a distorted-wave coupled channels code[32] and using an octupole deformability parameter $\beta_3=0.11$. The optical-model parameters used in the calculation are given in the caption and give very good fits to the elastic data (similar to the fits of Fig. 6). The value chosen for β_3 is in the region expected[33] for ^{208}Pb: A value of $\beta_3=0.20$ increases the cross section by about 20%. The total cross section from the direct nuclear scattering is very small. The point at issue here is the energy variation of the direct nuclear cross section rather than the precise numerical value, although the values in Fig. 8 should be a good guide. We will argue (in Sec. IV B) that $d\sigma_{\rm dn}$ falls off so rapidly with energy that it is most improbable that it is affecting the 18-MeV angular distribution significantly. The contribution of the compound-nucleus cross section $d\sigma_{\rm cn}$ to the inelastic α channel was estimated, by a rough Hauser-Feshbach calculation, to be about four times less than $d\sigma_{\rm dn}$ at $E_\alpha=19$ MeV ($\lesssim 1\%$ of $d\sigma^{(1)}$) and also to have about the same energy dependence as $d\sigma_{\rm dn}$. The direct nuclear amplitude will influence the Coulomb-excitation amplitude coherently, whereas $d\sigma_{\rm cn}$ will add incoherently to the final cross section.

We conclude that at 19 MeV the direct nuclear reaction is strongly affecting the inelastic α channel, and we present the 19-MeV results here in order to make the case (see Sec. IV B) that the energy variation of $d\sigma_{\rm dn}$ and $d\sigma_{\rm cn}$ and their approximate values is such that their influence at the lower two α energies can be safely neglected. It is useful to point out, however, that 19-MeV α's on ^{208}Pb would have been considered a "safe" bombarding energy for Coulomb-excitation experiments on the basis of a classical prescription for such "safe" energies.[1]

[32] T. Tamura, Rev. Mod. Phys. **37**, 679 (1965).
[33] G. R. Satchler, R. H. Bassel, and R. M. Drisko, Phys. Letters **5**, 256 (1963).

B. 18-MeV and 17.5-MeV α Data

The elastic scattering cross section differs from Rutherford at back angles by less than 3% at 18 MeV and less than 2% at 17.5 MeV (Fig. 6). Thus at these energies the effect of the compound-nucleus formation is still being felt in the elastic channel, and the question arises whether the inelastic data, shown in Figs. 9 and 10, can be analyzed in terms of pure Coulomb excitation. We note the following two arguments:

(i) The energy variation of the direct nuclear inelastic scattering $d\sigma_{\rm dn}$, given in Fig. 8 and discussed in detail in Sec. IV A, is very strong; it decreases about 10 times more rapidly than the Coulomb-excitation cross section as the energy is decreased, and so we expect that the small nuclear interference present at 19 MeV is most probably negligible at 18 and at 17.5 MeV.

(ii) The 18- and 17.5-MeV sets of inelastic data can be consistently analyzed in terms of electric excitation alone. Any significant interference from other amplitudes at these two bombarding energies would make this a most unlikely occurrence.

When the elastic scattering [or, more precisely, the sum of the elastic scattering and the Coulomb-excited inelastic scattering Eq. (1)] shows deviations from Rutherford scattering, one has to present convincing evidence that the mechanism responsible for the inelastic process is electric excitation alone. Classical criteria[1] and even the presence of (small) deviations[34] from pure Coulomb scattering, while being useful guides, may not adequately describe any specific experimental case which, ideally, should be decided by experiment, as we have attempted to do above. There remains a further question concerning the calculation of the theoretical Coulomb-excitation cross section $d\sigma_{\rm ce}$. In the semiclassical theory the probability of excitation along a classical orbit is calculated by perturbation theory

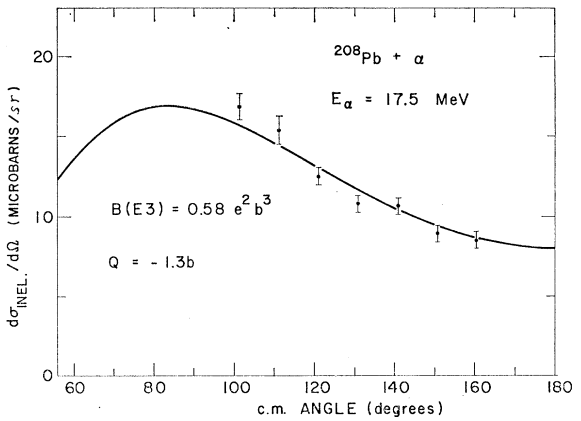

FIG. 10. Absolute angular distributions of the inelastic α scattering cross section to the 3^- ^{208}Pb state at 17.5-MeV incident energy. The best-fit parameters are $B(E3)\uparrow=0.58e^2$ b^3 and $Q=-1.3$ b (see the caption to Fig. 9).

[34] M. Samuel and U. Smilansky, Phys. Letters **28B**, 318 (1968).

[Eq. (1)] and then multiplied by the Rutherford scattering cross section. If the measured elastic scattering deviates from the Rutherford value, does one use $d\sigma_{\text{Ruth}}$ or $d\sigma_{\text{el}}$ in the formula for $d\sigma_{\text{ce}}$? The question loses its directness when the semiclassical expressions are symmetrized, for then the Rutherford orbit itself is symmetrized and no longer describes the experimental elastic scattering, even in the case of very small inelastic and no nuclear effects. We have taken the view that the theory predicts an absolute cross section for excitation and not the probability for excitation along a fictitious orbit, and we thus have compared the theoretical and experimental absolute differential cross sections. In most experimental situations in which the mechanism has been shown to be Coulomb excitation alone, the elastic scattering will not deviate more than a few percent from pure Coulomb. In the present experiment, the maximum deviation is $\sim 3\%$ at back angles for $E_\alpha = 18$ MeV, and the accuracy of the data makes the discussion rather academic. When the point becomes more important it will be necessary to develop and use a more accurate theory of the Coulomb-excitation process.

C. 69.1-MeV ^{16}O Data

At an oxygen bombarding energy of 69.1 MeV, the scattering is several MeV below the usual prescriptions for a Coulomb-barrier height and may be expected to be purely Rutherford. Figure 11 shows this to be the case to within a fraction of 1%. This, of course, does not prove that there is no nuclear interference in the inelastic cross section, although the comparison with the 18-MeV α data, where the inelastic channel was all Coulomb excitation even with 3% deviations from Rutherford, does make it plausible. The fact that nuclear-tunnelling cross sections are comparable with the inelastic scattering (Sec. II and Fig. 4) in no way suggests that direct nuclear inelastic processes may be important, since nuclear tunnelling can take place even when the ^{16}O sees effectively none of the tail of the ^{208}Pb nuclear potential. The inelastic cross section is plotted in Fig.

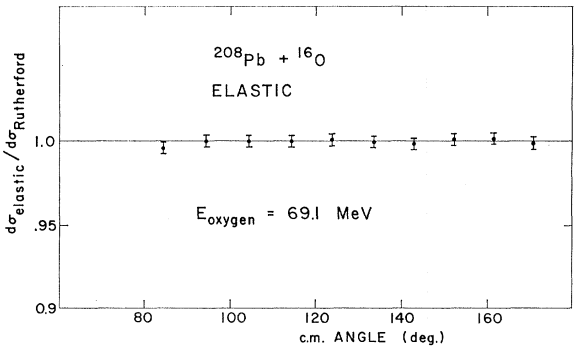

FIG. 11. Elastic oxygen angular distribution at 69.1-MeV bombarding energy given as a ratio to the Rutherford value. Since the ratio is constant, we assume that the scattering is described by the Rutherford value: The deduced target thickness is 59 μg/cm^2. Statistical and systematic errors amount to $\pm 0.3\%$.

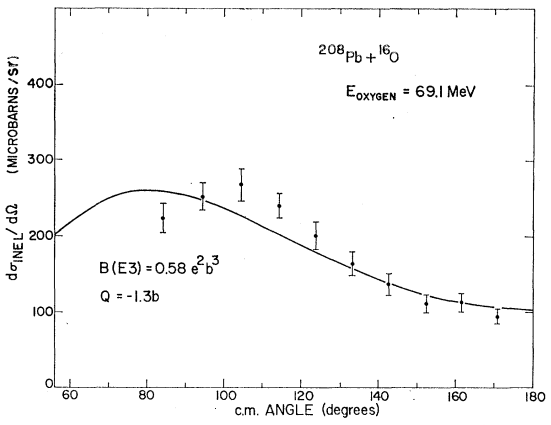

FIG. 12. Absolute angular distribution for inelastic scattering of oxygen ions with incident energy of 69.1 MeV, resulting in the Coulomb excitation of the 2.614-MeV octupole state of ^{208}Pb. The curve is calculated with the best-fit parameters $B(E3) = 0.58e^2\,\text{b}^3$ and $Q = -1.3$ b (see the caption to Fig. 9). The deviation from the first-order cross section provides a measure of Q (see Fig. 5).

12; the data, together with the 18- and 17.5-MeV α data, were analyzed on the assumption of pure Coulomb excitation, as is described in Sec. IV D.

While we believe it is true in the case of ^{208}Pb that no other second-order Coulomb-excitation paths are contributing significantly to the cross section [and so we can use Eq. (12) as a good approximation to the second-order perturbation theory], the ^{16}O experiment poses a problem that so far has not been treated in the literature. The single-nucleon-tunnelling cross sections at the back angles are comparable to the octupole Coulomb-excitation cross section. How important are virtual second-order processes involving two nuclear tunnellings which leave ^{208}Pb in its 3^- level, compared with the second-order Coulomb-excitation term we consider? This problem is present in $E2$ reorientation experiments also but probably to a lesser degree on account of the larger $E2$ cross sections. For the present, we assume that the two nucleon exchange contribution is not important.[35]

D. Least-Squares Analysis

The three sets of inelastic scattering data, Figs. 9, 10, and 12 were analyzed together in terms of the expression [Eq. (12)]

$$d\sigma(\theta) = B(E3)A(\theta)[1+QB(\theta)],$$

which was derived and discussed in Sec. III. The quantities $A(\theta)$ and $B(\theta)$ can be evaluated for the different ions and bombarding energies; they were calculated at 10° intervals and were interpolated to the actual c.m. angle of observation before being compared to the ex-

[35] Repeating the measurements with different bombarding energies and projectiles would help resolve this question and many others that occur in this type of measurement, as we have emphasized. The problem is of course one of the time available: The data presented here were obtained during 420-h use of an MP Tandem.

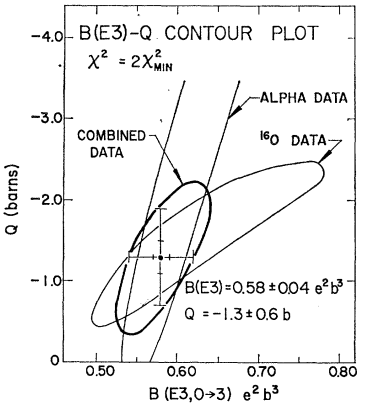

FIG. 13. *A* χ^2 analysis of the combined data of Figs. 9, 10, and 12. The curves define regions in $B(E3)$ and Q space for which the χ^2 value of the fit to the data is less than $2\chi^2_{\min}$, where $\chi^2_{\min}$ is the minimum χ^2 value of the data set. Pairs of points outside the curves show a distinctly inferior fit. Note the large range of Q over which the α data can be fitted, and that even the sign of Q is uncertain: $B(E3)_\alpha$ has the value 0.60 ± 0.07 e^2 b^3. The oxygen data alone define a large region of $B(E3)$-Q space which can be characterized by the ranges $B(E3)_{\text{oxygen}}=0.62\pm0.14$ e^2 b^3 and $Q_{\text{oxygen}}=-1.5\pm1.0$ b. Combining the α data with the oxygen data restricts the allowed range considerably, to the values quoted. The small error bars on the figure are the results of a least-square analysis (Sec. IV D): We feel they are unrealistically optimistic.

perimental values. The usual least-squares analysis was made in terms of the two parameters $B(E3)$ and $[B(E3)Q]$ and yielded the results

$$B(E3)_{\text{ls}}=0.58\pm0.01\ e^2\ \text{b}^3 \quad \text{and} \quad Q_{\text{ls}}=-1.34\pm0.17\ \text{b}.$$

The correlation coefficient[36] is $\rho=-0.790$, indicating, as expected, the high degree of correlation between the two parameters $B(E3)$ and $[B(E3)Q]$. The value of χ^2 is 32.3 for 26 data points, corresponding (if interpreted strictly) to a 15% confidence level relative to the expected $\chi^2=23$. We discuss the errors that we assign to $B(E3)$ and Q arising from the analysis, from the neglect of other terms in Eq. (12), and from theoretical uncertainties, in Sec. V.

V. DISCUSSION

The uncertainties in the values of $B(E3)$ and Q derived from our analysis are difficult to estimate. The errors obtained from the least-squares analysis of Sec. IV D are small, $B(E3)_{\text{ls}}=0.58\pm0.01$ e^2 b^3 and $Q_{\text{ls}}=-1.3\pm0.2$ b, and contain no allowance for the theoretical uncertainties in both the shape of the predicted angular distribution and in its magnitude. The minimum χ^2 value of this analysis, $\chi_{\min}^2$, is 32.3 with 26 data points. It is rather more informative to present the results of the analysis in an alternative way. Figure 13 shows curves defining the range of values of $B(E3)$ and Q for which the χ^2 of the data about the values of Eq. (12) is less than $2\chi_{\min}^2$. The theoretical curves for values of $B(E3)$ and Q outside this range show a marked visual worsening of the fits to the data. The results in Fig. 13 were obtained by calculating $\chi^2(B(E3), Q)$ over a grid of values indicated by the scales in the figure, $B(E3)=0.4(0.01)0.8$ and $(-Q)=0.0(0.2)4.0$. Only one minimum was found, identical to that of the least-squares analysis; however, it was quite shallow. If the intersections with the ellipse defined by $\chi^2=2\chi_{\min}^2$ are taken to give an estimate of the degree of confidence in the parameters, then we have

$$B(E3)=0.58\pm0.04\ e^2\ \text{b}^3 \quad \text{and} \quad Q=-1.3\pm0.6\ \text{b}.$$

It is evident that neither the α data nor the ^{16}O data alone give as precise estimates of the parameters: indeed, from the α ellipse of Fig. 13, one cannot even determine the sign of Q, let alone its magnitude. For the α data, it is clearly incorrect to assume that the first-order prediction (with $Q=0$) is sufficient to determine $B(E3)$ as accurately as the errors on the data would suggest. The oxygen data at least restrict Q to be negative, but the errors on the parameters are about three times those obtained using all the data.

The value of $\chi_{\min}^2/(N-3)$ is 1.40, so that, while the data set is not a very good statistical sample, it is not an unacceptable one. This consideration leads to a second source of error, not due to the experimental statistics, but related to the use of the simple expression (12). The most important terms ignored in Eq. (12) are $d\sigma^{(2)}$ and the unknown cross terms $d\sigma^{(1,3)}$, as discussed in Sec. III. The neglect of these terms will not influence the predictions of α particle excitation, but could affect the ^{16}O predictions by up to 5% (Table III). It is clearly possible that the inclusion of higher terms could significantly affect the value of Q derived from our experiments, but probably cause little change in $B(E3)$. [Including the $d\sigma^{(2)}$ terms and reevaluating the χ^2 grid, in fact, leads to $\chi_{\min}^2=32.8$ at the values $B(E3)=0.60$ and $Q=-2.0$, and to a curve which follows the α ellipse at larger values of Q, where the perturbation expression is invalid. The assessment of errors becomes essentially subjective.] We give our best estimate of the correlated parameters, using Eq. (12) for the theoretical values, as

$$B(E3)\uparrow=0.58\pm0.04\ e^2\,\text{b}^3 \quad \text{and} \quad Q=-1.3\pm0.6\ \text{b},$$

and believe that errors quoted are realistic.

There are several other measurements of the $B(E3)\uparrow$ for the upward transition from the ground state to the 3^- level. These range from 0.31 to 0.97 e^2 b^3, and stem from investigations that use a variety of experimental techniques and theoretical interpretations. Total Coulomb excitation cross sections derived from γ-ray measurements[37] following heavy ion bombardment of ^{208}Pb are subject to errors in the determination of the detector efficiency and in some measure to errors associated with the neglect of second-order terms in expressions for the total cross section. Measurements

[36] A. J. Ferguson, *Angular Correlation Methods in Gamma-Ray Spectroscopy* (North-Holland Publishing Co., Amsterdam, 1965), Chap. IV.

[37] A. Z. Hrynkiewicz, S. Kopta, S. Szymczyk, and T. Walczak, Nucl. Phys. **79**, 495 (1966).

involving distorted-wave Born approximation (DWBA) analyses of (p, p') and (α, α') experiments[38] are subject to the usual uncertainties of lack of precise knowledge of optical-model parameters and details of the reaction mechanism. Inelastic electron experiments are technically difficult and are involved in interpretation: $B(E3)$ values from such experiments range from[39] 0.54 e^2 b^3 to[40] 0.88 e^2 b^3, with a recent determination[15] of 0.72 ± 0.04 e^2 b^3. A good measurement of the lifetime of the 3^- state would provide an unambiguous value for the upward $B(E3)$ and would remove some uncertainty from the value of Q obtained in this experiment. The lifetime is around 25 psec and is in a region where accurate measurements are difficult. The only lifetime value reported[41] gives a preliminary value of the mean life $\tau_m=47\pm15$ psec, equivalent to $B(E3)\uparrow=0.31$ e^2 b^2. The present measurement of $B(E3)\uparrow$ is the most direct one and probably gives the best available value.

Our results for $B(E3)\uparrow$ and Q may be compared with theoretical predictions. There exist a number of calculations on ^{208}Pb: To first order the levels are described by mixing a limited set of particle-hole configurations (of protons and neutrons separately) arising from excitations across the closed proton and neutron shells. In the more recent treatments, Letourneux and Eisenberg[42] use a surface δ-function force to mix the configurations, Gillet *et al.*[9] use more general residual nucleon-nucleon interactions, and Krainov[43] uses an interaction which is taken to vary with the density of the nucleons and which is different for the proton and neutron particle-hole pairs. In all of these calculations a 3^- level is depressed into the energy gap, and most of the octupole strength is concentrated on it. It proves necessary to include ground-state correlations in order to increase the $E3$ strength towards the observed value: In the first two of the above calculations this is done by using the random phase approximation, and in Krainov's work it is done by the use of a method[44] of treating the nucleus in an analogous fashion to the Landau theory of Fermi liquids.[45] In Refs. 9 and 42 the energy of the 3^- level is reproduced if many particle-hole configurations are included, but the $B(E3)$ for the transition to the 3^- state is about a factor of 2 too small. Krainov reproduces the energy of the level and finds $B(E3)\uparrow=25$ s.p.u. and $Q=-2.4$ s.p.u., but does not define these units. If we use the customary expression[4]

$$B(E\lambda, I_i\rightarrow I_f)_{\text{s.p.}}=B(E\lambda)_{\text{s.p.}}=(2\lambda+1)\frac{e^2}{4\pi}\left(\frac{3}{3+\lambda}\right)^2 R_0^{2\lambda}, \quad (13)$$

with $R_0=1.2A^{1/3}$ F, for the single-particle unit for the reduced transition matrix element, then our result for $B(E3)\uparrow$ is equal to 32 s.p.u. In an analogous manner to Eq. (9) we can define a quadrupole moment single-particle unit as

$$eQ_{\text{s.p.}}=(16\pi/5)^{1/2}[B(E2)\uparrow_{\text{s.p.}}(2I+1)]^{1/2}\times[I(2I-1)/(2I+1)(I+1)(2I+3)]^{1/2}, \quad (14)$$

i.e., $Q_{\text{s.p.}}=(\frac{3}{5})^{1/2}R_0^2$ for $I=3$. In terms of this result, our value of Q is equal to -3.0 s.p.u. It is clear that the particle-hole predictions are in reasonable agreement with the measurements.

In conclusion, we have described the measurement of the quadrupole moment of the 3^- octupole state in ^{208}Pb using the reorientation effect following Coulomb excitation by both α's and oxygen. In addition, we have determined the $B(E3)\uparrow$ matrix element for the transition from the ground state. The values for the quadrupole moment and the $B(E3)$ are correlated, our best values being

$$Q=-1.3\pm0.6 \text{ b} \quad \text{and} \quad B(E3)\uparrow=0.58\pm0.04 \ e^2 \text{ b}^3.$$

Even allowing for the difficulties of assigning errors, our value for Q is clearly not zero; we may note, however, that the observed value of Q does not imply a large deformation of the 3^- state. If we were to consider the system as an axially symmetric ellipsoid in the lowest state of a rotational band with $I=K=3$, then the intrinsic quadrupole moment Q_0 would be equal to -3.1 b. This would correspond to a deformation β of about 0.10, a value somewhat smaller than those associated with "rotational" nuclei. The nonzero quadrupole moment perhaps alters the macroscopic picture of the level as a pure-octupole-shape vibration in that the equilibrium shape can no longer be spherical.

ACKNOWLEDGMENTS

We would like to acknowledge the expert computing assistance and advice of R. Goodwin, the use of the optical-model code of F. Becchetti, Jr., the coupled-channels code of N. Lingappa, and the target preparation of G. Ott. We would like to thank G. W. Greenlees and D. R. Bes for their critical reading of the manuscript. W. R. Phillips wishes to acknowledge the hospitality of the Williams Laboratory during his stay in Minneapolis.

[38] J. Alster, Phys. Rev. **141**, 1138 (1966); Phys. Letters **25B**, 459 (1967); A. Scott and M. P. Fricke, *ibid.* **20**, 654 (1966); J. Saudinos, G. Vallois, O. Beer, M. Gerdrot, and P. Lopato, *ibid.* **22**, 492 (1966); G. R. Satchler, R. H. Bassel, and R. M. Drisko, *ibid.* **5**, 256 (1963); T. Stovall and N. M. Hintz, Phys. Rev. **135**, B330 (1964).

[39] H. Kendall and J. Oeser, Phys. Rev. **130**, 245 (1963).

[40] D. S. Onley, J. T. Reynolds, and L. E. Wright, Phys. Rev. **134**, B945 (1964).

[41] R. S. Weaver, Can. J. Phys. **40**, 1684 (1962).

[42] J. Letourneux and J. M. Eisenberg, Nucl. Phys. **85**, 119 (1966).

[43] V. P. Krainov, Phys. Letters **27B**, 341 (1968).

[44] A. B. Migdal, Zh. Eksperim. i Teor. Fiz. **43**, 1940 (1962) [English transl.: Soviet Phys.—JETP **16**, 1366 (1963)]; A. J. Larkin and A. B. Migdal, Zh. Eksperim. i Teor. Fiz. **44**, 1703 (1963) [English transl.: Soviet Phys.—JETP **17**, 1146 (1963)]; A. B. Migdal and A. J. Larkin, Nucl. Phys. **51**, 561 (1964); A. B. Migdal and A. J. Larkin, Zh. Eksperim. i Teor. Fiz. **45**, 1036 (1963) [English transl.: Soviet Phys.—JETP **18**, 717 (1964)].

[45] L. D. Landau, Zh. Eksperim. i Teor. Fiz. **35**, 97 (1958) [English transl.: Soviet Phys.—JETP **8**, 70 (1959)].